Chapter 5

Structure and spectra of polyatomic molecules

5.1 Structure of polyatomic molecules

The same approximations can be used for the stationary states of a polyatomic molecule as for a diatomic molecule, in particular the approximate separability of the motions and the Born-Oppenheimer approximation discussed in Chapter 3.

5.1.1 Rotational Structure

The rotational energy level structure of a molecule can be determined by analyzing the rotational motion classically and then, by using the correspondence principle, to determine the Hamilton operator $\hat{H}_{\text{rot}}$ and finally, by determining the eigenfunctions and eigenvalues of $\hat{H}_{\text{rot}}$.

Angular velocity, angular momentum and inertial tensor

Let us consider a rigid rotor. Each particle i of the rotor has the same angular velocity $|\vec{\omega}|$ around an axis passing through the center of mass (CM) as shown in Figure 5.1.

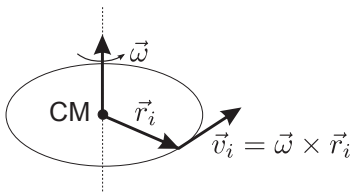

Figure 5.1: Angular velocity $\vec{\omega}$.

The angular momentum is

$$\vec{J} = \sum_{i=1}^{N} m_i \left(\vec{r}_i \times \vec{v}_i\right) = \sum_{i=1}^{N} m_i [\vec{r}_i \times (\vec{\omega} \times \vec{r}_i)]. \tag{5.1}$$

Using $\vec{v}_1 \times (\vec{v}_2 \times \vec{v}_3) = (\vec{v}_1 \cdot \vec{v}_3)\, \vec{v}_2 - (\vec{v}_1 \cdot \vec{v}_2)\, \vec{v}_3$, Equation (5.1) can be rewritten as

$$\vec{J} = \sum_{i=1}^{N} m_i [\vec{\omega}\, \vec{r}_i^{\,2} - \vec{r}_i (\vec{r}_i \cdot \vec{\omega})] \tag{5.2}$$

with $\vec{r}_i \cdot \vec{\omega} = x_i\omega_x + y_i\omega_y + z_i\omega_z$. Thus:

$$J_x = \left[\sum_i m_i (r_i^2 - x_i^2)\right] \omega_x - \left[\sum_i m_i x_i y_i\right] \omega_y - \left[\sum_i m_i x_i z_i\right] \omega_z, \tag{5.3}$$

$$J_y = -\left[\sum_i m_i x_i y_i\right] \omega_x + \left[\sum_i m_i (r_i^2 - y_i^2)\right] \omega_y - \left[\sum_i m_i y_i z_i\right] \omega_z, \tag{5.4}$$

$$J_z = -\left[\sum_i m_i x_i z_i\right] \omega_x - \left[\sum_i m_i y_i z_i\right] \omega_y + \left[\sum_i m_i (r_i^2 - z_i^2)\right] \omega_z. \tag{5.5}$$

One can express Equations (5.3)–(5.5) in matrix notation:

$$\vec{J} = \boldsymbol{I} \cdot \vec{\omega} \tag{5.6}$$

$$\begin{pmatrix} J_x \\ J_y \\ J_z \end{pmatrix} = \begin{pmatrix} I_{xx} & I_{xy} & I_{xz} \\ I_{yx} & I_{yy} & I_{yz} \\ I_{zx} & I_{zy} & I_{zz} \end{pmatrix} \begin{pmatrix} \omega_x \\ \omega_y \\ \omega_z \end{pmatrix} \tag{5.7}$$

with

$$\begin{aligned} I_{\alpha\alpha} &= \sum_i m_i (r_i^2 - \alpha_i^2) \\ I_{\alpha\beta} &= -\sum_i m_i \alpha_i \beta_i, \end{aligned} \tag{5.8}$$

whereby $\alpha,\ \beta = x, y, z$. The matrix $\boldsymbol{I}$ is real and symmetric.

A unitary transformation can bring $\boldsymbol{I}$ in diagonal form with diagonal elements I_a, I_b, I_c where a, b, c are the principal axes of the rigid rotor. I_a, I_b and I_c are the roots of the determinantal equation:

$$\begin{vmatrix} I_{xx} - \lambda & I_{xy} & I_{xz} \\ I_{yx} & I_{yy} - \lambda & I_{yz} \\ I_{zx} & I_{zy} & I_{zz} - \lambda \end{vmatrix} = 0\ . \tag{5.9}$$

Convention: The principal axes are labelled a, b and c so that

$$I_a \leq I_b \leq I_c\,. \tag{5.10}$$

The angular momentum components in the principal axis system are

$$\begin{aligned} J_a &= I_a\omega_a \ , \\ J_b &= I_b\omega_b \ , \\ J_c &= I_c\omega_c \ . \end{aligned} \tag{5.11}$$

Classification of rotors

Molecules can be classified into different types of rotors depending on the relation between the three diagonal components of the moment of inertia.

$I_a = 0, I_b = I_c$	:	linear molecule
$I_a < I_b = I_c$	:	prolate symmetric top with the shape of a "rugby ball", see Figure 5.2 (example: CH_3Cl)
$I_a = I_b < I_c$	:	oblate symmetric top with the shape of a "disc", see Figure 5.2 (example: benzene)
$I_a = I_b = I_c = I$	:	spherical top (examples: CH_4, C_{60})
$I_a < I_b < I_c$	:	asymmetric top (example: H_2O)

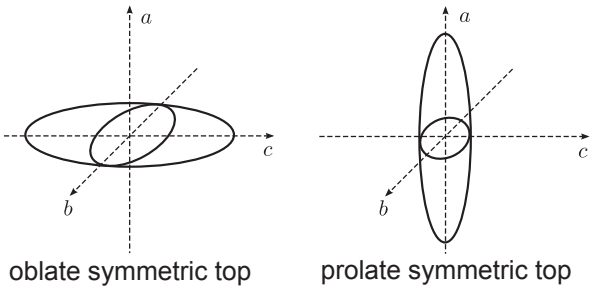

Figure 5.2: Scheme of oblate and prolate symmetric top rotors.

Moreover, for planar molecules:

$$I_a + I_b = I_c \tag{5.12}$$

Rigid rotor energy levels

The classical kinetic energy of a rotor is:

$$\begin{aligned} T &= \frac{1}{2}\sum_i m_i v_i^2 = \frac{1}{2}\sum_i m_i\, \vec{v}_i(\vec{\omega}\times\vec{r}_i) = \frac{1}{2}\vec{\omega}\sum_i m_i(\vec{r}_i\times\vec{v}_i) = \frac{1}{2}\,\vec{\omega}\cdot\vec{J} \\ &= \frac{1}{2}\left[\omega_a^2 I_a + \omega_b^2 I_b + \omega_c^2 I_c\right] = \frac{J_a^2}{2I_a} + \frac{J_b^2}{2I_b} + \frac{J_c^2}{2I_c}\,. \end{aligned} \tag{5.13}$$

According to the correspondence principle, the Hamiltonian for a rigid rotor is therefore

$$\hat{H}_{\text{rot}} = \frac{\hat{J}_a^2}{2I_a} + \frac{\hat{J}_b^2}{2I_b} + \frac{\hat{J}_c^2}{2I_c}. \tag{5.14}$$

The quantum mechanical description of the rotational motion of a rotor requires three quantum numbers because there are three degrees of freedom associated with the rotation in free space. We use the following quantum numbers: J the rotational quantum number, M the quantum number associated with the projection of $\vec{J}$ onto the space-fixed Z axis and K the quantum number associated with the projection of $\vec{J}$ onto the z axis of the molecule-fixed reference frame. With these notations, the wave functions $|J\,K\,M\rangle$ are eigenfunctions of $\hat{J}^2$ and $\hat{J}_z$.

The rotational constants A, B and C are defined as

$$\begin{aligned} \frac{\hbar^2}{2I_a} &= hcA, \\ \frac{\hbar^2}{2I_b} &= hcB\,, \text{ and} \\ \frac{\hbar^2}{2I_c} &= hcC\,. \end{aligned} \tag{5.15}$$

With this definition the rotational constants are expressed in cm^{-1}. In the following we will simplify the expression of the rotational energy, when possible, for each specific case of rotors (see also lecture notes Physical Chemistry III).

Spherical top: $I_a = I_b = I_c$

Equation (5.14) becomes

$$\hat{H}_{\text{rot}} = \frac{\hat{J}^2}{2I}\,, \tag{5.16}$$

$$\begin{aligned} \hat{H}_{\text{rot}}|J\,K\,M\rangle &= E_J\,|J\,K\,M\rangle \\ \frac{1}{2I}\hat{J}^2|J\,K\,M\rangle &= \underbrace{\frac{\hbar^2}{2I}J(J+1)}_{\text{Eigenvalue}}|J\,K\,M\rangle\,. \end{aligned} \tag{5.17}$$

The eigenvalues for the rotational motion of a spherical top are

$$E_J = \frac{\hbar^2}{2I}J(J+1)\,. \tag{5.18}$$

The spectroscopic usage is to write $E_J = hcBJ(J+1)$ with $B = \frac{\hbar^2}{2hcI}$. The energy does not depend on K or M and each level has a degeneracy factor $g = (2J+1)(2J+1)$.

Oblate symmetric top: $I_a = I_b < I_c$.

The axes will be chosen as follows: $a \leftrightarrow x$, $b \leftrightarrow y$, $c \leftrightarrow z$. Equation (5.14) becomes

$$\begin{aligned} \hat{H}_{\rm rot}|J\,K\,M\rangle &= \left[\frac{1}{2I_b}(\hat{J}_x^2+\hat{J}_y^2)+\frac{1}{2I_c}\hat{J}_z^2\right]|J\,K\,M\rangle \\ &= \left[\frac{1}{2I_b}(\hat{J}^2-\hat{J}_z^2)+\frac{1}{2I_c}\hat{J}_z^2\right]|J\,K\,M\rangle \\ &= \underbrace{hc\left\{BJ(J+1)+(C-B)K^2\right\}}_{\text{Eigenvalue}}|J\,K\,M\rangle \end{aligned} \tag{5.19}$$

with $B > C$. The degeneracy is $g_{J,0} = 2J+1$ for $K = 0$ and $g_{J,K} = 2(2J+1)$ for $K \neq 0$.

Prolate symmetric top: $I_a < I_b = I_c$

The axes will be chosen as follows: $a \leftrightarrow z$, $b \leftrightarrow x$, $c \leftrightarrow y$. Equation (5.14) becomes

$$\hat{H}_{\rm rot}|J\,K\,M\rangle = \left[\frac{1}{2I_b}(\hat{J}^2-\hat{J}_z^2)+\frac{1}{2I_a}\hat{J}_z^2\right]|J\,K\,M\rangle = hc\left\{BJ(J+1)+(A-B)K^2\right\}|J\,K\,M\rangle \tag{5.20}$$

with $A > B$. The degeneracy is $g_{J,0} = 2J+1$ for $K = 0$ and $g_{J,K} = 2(2J+1)$ for $K \neq 0$.

Diatomic molecule:

The case of diatomic molecules (already seen in Chapter 3) can be considered as a special case of prolate top with $A = \infty$. Hence $K = 0$.

$$E_{JKM} = hcBJ(J+1) \tag{5.21}$$

with a degeneracy of $g_J = 2J+1$. Figure 5.3 summarizes the rotational level structure of the four specific rotors discussed.

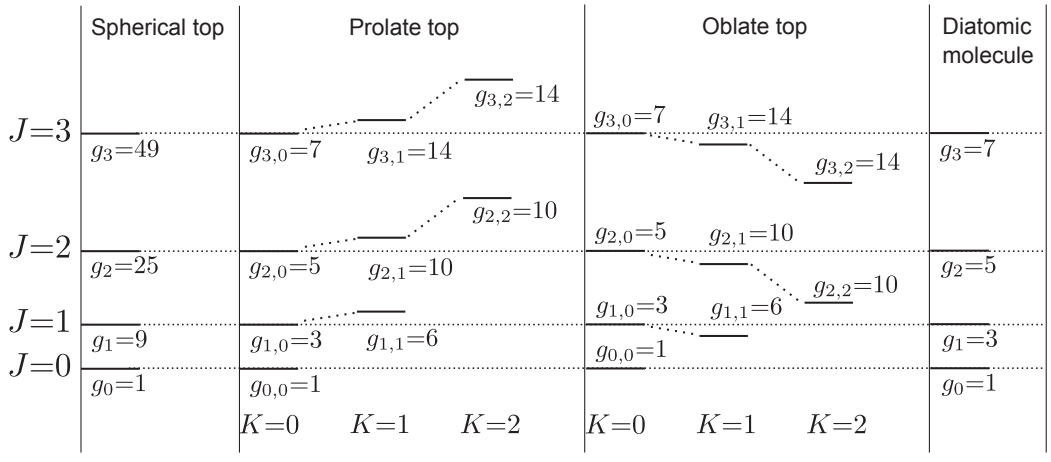

Figure 5.3: Schematic diagram representing the rotational level structure of different rotors. The diagram also includes the degeneracy g of the rotational levels. Levels with $K \geq J$ do not exist.

Asymmetric top: $I_a \neq I_b \neq I_c$

The $|J\,K\,M\rangle$ functions are not eigenfunctions of $\hat{H}_{\rm rot}$. However, they form a complete set of basis functions and the wave functions $|J\,\tau\,M\rangle$ of an asymmetric top can be represented as a linear combination of these basis functions:[a]

$$|J\,\tau\,M\rangle = \sum_{K=-J}^{J} c_{\tau,K}|J\,K\,M\rangle \tag{5.22}$$

To obtain the energy levels of an asymmetric top, the following procedure can be followed: one constructs $\hat{H}_{\rm rot}$ in matrix form and obtains the energies by looking for the eigenvalues of $\hat{H}_{\rm rot}$ (after diagonalization of the matrix).

$$\hat{H}_{\rm rot} = \frac{1}{2I_a}\hat{J}_a^2 + \frac{1}{2I_b}\hat{J}_b^2 + \frac{1}{2I_c}\hat{J}_c^2 \tag{5.23}$$

Example: construction of the matrix representation of $\hat{J}_z$ and $\hat{J}_z^2$ in the $\{|J\,K\,(M)\rangle\}$ basis for $J = 1$: $\{|1\,1\rangle\,|1\,0\rangle\,|1\ -1\rangle\}$

$\hat{J}_z$	$\lvert 11\rangle$	$\lvert 10\rangle$	$\lvert 1-1\rangle$
$\langle 11\rvert$	$\hbar$	0	0
$\langle 10\rvert$	0	0	0
$\langle 1-1\rvert$	0	0	-$\hbar$

$\hat{J}_z^2$	$\lvert 11\rangle$	$\lvert 10\rangle$	$\lvert 1-1\rangle$
$\langle 11\rvert$	$\hbar^2$	0	0
$\langle 10\rvert$	0	0	0
$\langle 1-1\rvert$	0	0	$\hbar^2$

The matrix elements are calculated in the following way:

$(J_z)_{11} = \langle 1\,1|\hat{J}_z|1\,1\rangle = \langle 1\,1|\hbar K|1\,1\rangle = \hbar K\langle 11|11\rangle = \hbar K = \hbar$

$(J_z)_{12} = \langle 1\,1|\hat{J}_z|1\,0\rangle = \langle 1\,1|0|1\,0\rangle = 0\underbrace{\langle 1\,1|1\,0\rangle}_{0} = 0\cdot 0 = 0$

$(J_z)_{22} = \langle 1\,0|\hat{J}_z|1\,0\rangle = \langle 1\,0|0|1\,0\rangle = 0$

$(J_z)_{33} = \langle 1\ -1|\hat{J}_z|1\ -1\rangle = \langle 1\ -1|-\hbar|1\ -1\rangle = -\hbar\langle 1\ -1|1\ -1\rangle = -\hbar$

---

[a] Note that τ is not a good quantum number but simply an index running from $-J$ to J with the associated energy levels $E_{J\,\tau}$ arranged in ascending order. In the literature, the double index K_a, K_c is used instead of τ, where K_a and K_c represent K in the prolate top and oblate top limiting case, respectively; $\tau = K_a - K_c$.

5.1.2 Vibrational Structure

The number of vibrational degrees of freedom is $f = 3N - 6$ for a nonlinear molecule, and $f = 3N - 5$ for a linear molecule.

In the treatment of the vibrational motion of a polyatomic molecule, one makes use of the near-separability of the nuclear Schrödinger equation in the normal modes. The starting point is

$$\hat{H} = \sum_{i=1}^{3N} \frac{\hat{p}_i^2}{2m_i} + V(x_1, \ldots, z_N). \tag{5.24}$$

One introduces mass-weighted displacement coordinates

$$q_i = \sqrt{m_i}\Delta x_i = \sqrt{m_i}\,(x_i - x_i^{\mathrm{eq}}), \tag{5.25}$$

so that

$$\hat{T} = \frac{1}{2}\sum_{i=1}^{3N} \dot{q}_i^2. \tag{5.26}$$

The potential is then expanded around the equilibrium position (eq) in a Taylor series:

$$V = V_{\mathrm{eq}} + \underbrace{\sum_{i=1}^{3N} \left(\frac{\partial V}{\partial q_i}\right)_{\mathrm{eq}} q_i}_{0\,\text{at the minimum}} + \frac{1}{2}\sum_{i=1}^{3N}\sum_{j\geq i}^{3N} \left(\frac{\partial^2 V}{\partial q_i \partial q_j}\right)_{\mathrm{eq}} q_i q_j + \ldots \tag{5.27}$$

Harmonic vibrations

Setting $V_{\mathrm{eq}} = 0$ and making the harmonic approximation, Equations (5.24) and (5.27) simplify to

$$\hat{H} = \hat{T} + \frac{1}{2}\sum_{i=1}^{3N}\sum_{j\geq i}^{3N} k_{ij}\, q_i\, q_j\,, \tag{5.28}$$

with

$$k_{ij} = \left(\frac{\partial^2 V}{\partial q_i \partial q_j}\right)_{\mathrm{eq}}. \tag{5.29}$$

By a suitable basis transformation and separation of the rotational and translational motion one obtains the normal modes Q_k as linear combination of the displacement coordinates:

$$Q_k = \sum_{i=1}^{3N} L_{ik}\, q_i \quad k = 1, 2, ..., 3N - 6, \tag{5.30}$$

where L_{ik} represent the expansion coefficients. The normal modes form an orthogonal set and $\hat{H}$ can be written as a sum of terms acting only on the coordinate Q_k

$$\hat{H} = \sum_{i=1}^{3N-6} \left(\frac{1}{2}\dot{Q}_i^2 + \frac{1}{2}\lambda_i Q_i^2\right). \tag{5.31}$$

Because $\hat{H}$ is separable in the normal modes, one can write the solution of the Schrödinger equation as

$$E_{v_1,v_2,...,v_{3N-6}} = \sum_{i=1}^{3N-6} h\nu_i \left(v_i + \frac{1}{2}\right) \tag{5.32}$$

$$\Psi_{v_1,v_2,...,v_{3N-6}} = \Psi_{v_1}(Q_1)\ \Psi_{v_2}(Q_2) ...\ \Psi_{v_{3N-6}}(Q_{3N-6}). \tag{5.33}$$

Example: triatomic molecules ($N = 3$)

The number of degrees of freedom is 3 for SO_2 and 4 for CO_2.

In CO_2 the bending mode is doubly degenerate (see Figure 5.4). The excitation of a degenerate vibrational mode leads to a vibrational angular momentum $\vec{l}$. In CO_2 this angular momentum is parallel to the molecular axis (see Figure 5.5) and corresponds to a superposition of motion in the two degenerate bending modes.

$|\vec{l}| = l_z = \hbar l$ with $l = -v_2, v_2 + 2, ..., v_2$. The total angular momentum is

$$\vec{J} = \vec{J}_{\mathrm{R}} + \vec{l} \tag{5.34}$$

and thus

$$E_{\mathrm{rot}} = hcBJ_{\mathrm{R}}(J_{\mathrm{R}} + 1) = hcB[J(J + 1) - l^2] \tag{5.35}$$

Anharmonic vibrations

Taking higher terms in Equation (5.27) one gets:

$$V = V_0 + \frac{1}{2}\sum_{i=1}^{3N}\sum_{j\geq i}^{3N} k_{ij}\, q_i\, q_j + \frac{1}{3!}\sum_{i=1}^{3N}\sum_{j\geq i}^{3N}\sum_{k\geq j}^{3N} k_{ijk}\, q_i\, q_j\, q_k + ... \tag{5.36}$$

and

$$T(v_1, ..., v_{3N-6}) = \frac{E_{v_1,...,v_{3N-6}}}{hc} = \sum_i \omega_i \left(v_i + \frac{d_i}{2}\right) + \sum_i \sum_{j\geq i} x_{ij} \left(v_i + \frac{d_i}{2}\right)\left(v_j + \frac{d_i}{2}\right) + ...$$
$$+ \sum_{\text{degenerate modes}\, i\leq l} g_{ij} l_i l_j \tag{5.37}$$

where d_i is the degree of degeneracy of the vibrational mode i. The constants ω_i and x_{ij} are given in cm^{-1} in Equation (5.37).

Example: CO_2

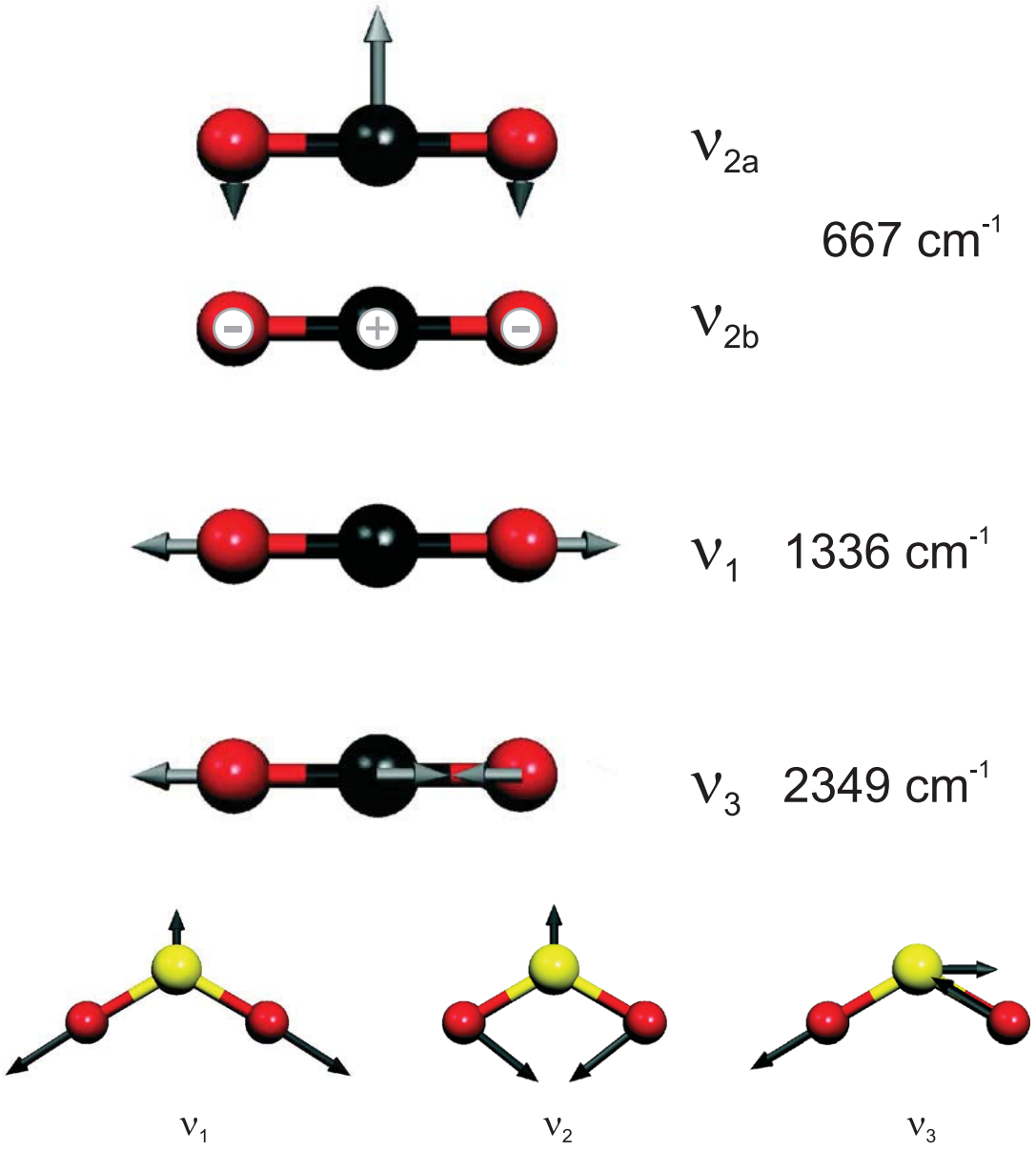

Figure 5.4: Schematic representation of the normal modes of CO_2 (top) and SO_2 (bottom).

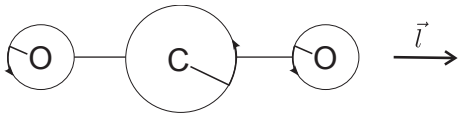

Figure 5.5: Vibrational angular momentum $\vec{l}$ of CO_2

$\omega_1 = 1354.07\ \mathrm{cm}^{-1}$, $\omega_2 = 672.95\ \mathrm{cm}^{-1}$, $\omega_3 = 2396.30\ \mathrm{cm}^{-1}$, $x_{11} = -3.1\ \mathrm{cm}^{-1}$, $x_{22} = -1.59\ \mathrm{cm}^{-1}$,

$x_{33} = -12.5$ cm^{-1}, $x_{12} = -5.37$ cm^{-1}, $x_{13} = -19.27$ cm^{-1}, $x_{23} = -12.51$ cm^{-1}, $g_{22} = -0.62$ cm^{-1}.

$$\begin{aligned} T(v_1, v_2, v_3) &= \omega_1 \left(v_1 + \frac{1}{2}\right) + \omega_2(v_2 + 1) + \omega_3 \left(v_3 + \frac{1}{2}\right) \\ &\quad + x_{11} \left(v_1 + \frac{1}{2}\right)^2 + x_{22}(v_2 + 1)^2 + x_{33} \left(v_3 + \frac{1}{2}\right)^2 \\ &\quad + x_{12} \left(v_1 + \frac{1}{2}\right)(v_2 + 1) + x_{13} \left(v_1 + \frac{1}{2}\right)\left(v_3 + \frac{1}{2}\right) + x_{23}(v_2 + 1)\left(v_3 + \frac{1}{2}\right) \\ &\quad + g_{22} l_2^2 \end{aligned} \tag{5.38}$$

The zero point vibrational energy contains a contribution from the anharmonicity terms ($l = 0$ for $v_2 = 0$)

$$T(0, 0, 0) = \frac{\omega_1}{2} + \omega_2 + \frac{\omega_3}{2} + \frac{x_{11}}{4} + x_{22} + \frac{x_{33}}{4} + \frac{x_{12}}{2} + \frac{x_{13}}{4} + \frac{x_{23}}{2}. \tag{5.39}$$

5.1.3 Molecular orbitals, electronic configurations, and electronic states

The electronic structure of polyatomic molecules can be described using the same principles as those introduced for diatomic molecules in chapter 3. However, the same polyatomic molecule can have different geometries and belongs to different point groups depending on its electronic state. The variety of possible electronic states and molecular structures is so large that it is impossible to give a complete overview in this chapter. We therefore restrict the discussion to only a few representative molecular systems: Molecules of the form HAH as prototypical small molecules, the cyclopentadienyl cation and benzene as typical highly symmetrical molecules and adenine as example of a nonsymmetrical large molecule. The principles that we describe are easily generalized to arbitrary molecules.

Small polyatomic molecules with the example of HAH molecules

Molecules possessing the chemical formula HAH (A designates an atom, *e. g.*, Be, B, C, N, O, etc.) are either linear and belong to the $D_{\infty h}$ point group (see character table in Chapter 4), or bent and belong to the C_{2v} point group (see character table 5.1). Molecular orbitals are therefore classified either in the $D_{\infty h}$ or the C_{2v} point group (see character tables in chapter 4). For simplicity we consider here only valence states of HAH molecules with A being an atom from the second or third row of the periodic table, so that $\ell \geq 2$ atomic orbitals can be ignored in the discussion of the electronic structure.

The determination of the molecular orbitals may proceed along the following scheme:

C_{2v}	E	C_2^z	σ_v^{xz}	σ_v^{yz}		
A_1	1	1	1	1	T_z	$\alpha_{xx}, \alpha_{yy}, \alpha_{zz}$
A_2	1	1	−1	−1	R_z	α_{xy}
B_1	1	−1	1	−1	T_x, R_y	α_{xz}
B_2	1	−1	−1	1	T_y, R_x	α_{yz}

Table 5.1: Character table of the C_{2v} point group.

1. Identification of all atomic orbitals participating in the formation of molecular orbitals. Symmetry restricts the number of these orbitals. In the case of HAH molecules, the required orbitals are the two 1s orbitals of the hydrogen atoms and the ns and np valence orbitals of the central atom A, where $n \geq 2$ represents the row of the periodic system of elements to which A belongs. Orbitals belonging to inner shells of the central atom usually lie so deep in energy and are so strongly localized on the nucleus that they hardly contribute to molecular bonds.

2. Formation of i symmetry-adapted molecular orbitals from the set of i atomic orbitals determined under (a) ($i = 6$ in the case of HAH molecules). Symmetry-adapted molecular orbitals transform as irreducible representations of the corresponding point group. In molecules such as HAH in which two or more atoms are equivalent, it is convenient to first build symmetry-adapted linear combinations of the orbitals of these equivalent atoms, *i. e.*, of the H 1s orbitals in the case of HAH molecules (see Figure 5.6).

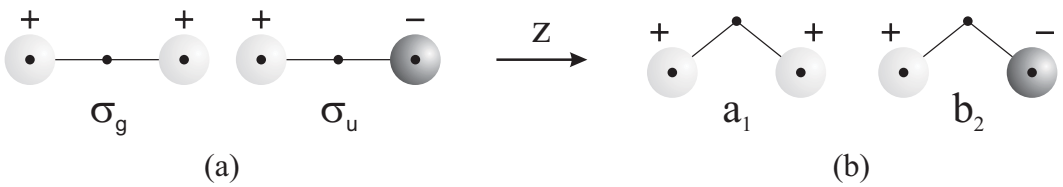

Figure 5.6: Symmetry adapted linear combinations of 1s orbitals that participate in the construction of molecular orbitals of (a) linear and (b) bent HAH molecules.

These orbitals are then used to form molecular orbitals with the orbitals of the central atom A having the corresponding symmetry, as shown in Figure 5.7 for the point group $D_{\infty h}$.

The ns (σ_g) and np$_z$ (σ_u) orbitals of the central atom can be combined with the symmetry-adapted orbitals of the H atoms in two ways each, resulting in four molecular orbitals of σ symmetry. The energetic ordering of these molecular orbitals can be derived from the num-

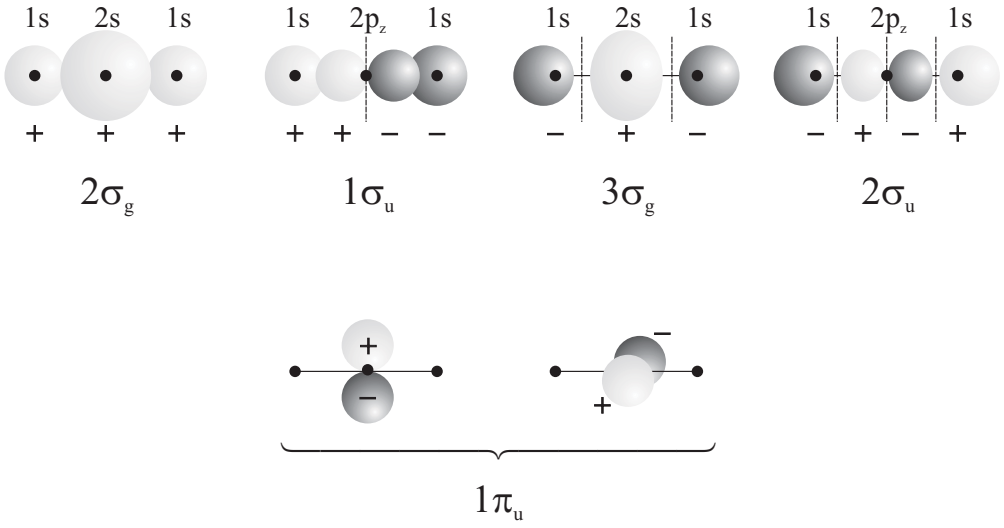

Figure 5.7: Linear combinations of atomic orbitals in linear HAH molecules

ber of nodal planes of the wave functions. The $2\sigma_g$ (zero nodal plane) and $1\sigma_u$ (one nodal plane) orbitals in Figure 5.7 are bonding, whereas the $3\sigma_g$ (two nodal planes) and $2\sigma_u$ (three nodal planes) orbitals are antibonding. For symmetry reasons, the $2p_x$ and $2p_y$ orbitals of the central atom (both of π_u symmetry) cannot combine with the 1s orbitals of the H atoms and are therefore nonbonding orbitals.

The energetic ordering of these molecular orbitals is given on the right-hand side of Figure 5.8 which also shows how the energies of the molecular orbitals change as the molecule is progressively bent from the linear $D_{\infty h}$ structure ($\angle$(HAH)= 180°) toward the C_{2v} structure with $\angle$(HAH)= 90°. The orbitals of the bent molecules displayed on the left-hand side of Figure 5.8 are given symmetry labels of the C_{2v} point group according to their transformation properties (see character table). The two lowest-lying orbitals are invariant under rotations around the C_2^z axis, and also under reflection in both the σ_{xz} and σ_{yz} planes, and are therefore totally symmetric (a_1). The next higher-lying orbital is antisymmetric under C_2 rotation and under σ_{xz} reflection, but symmetric under σ_{yz} reflection, and is thus of b_2 symmetry. As in the linear geometry, the energetic ordering essentially follows the number of nodal planes.

The degeneracy of the two nonbonding π_u orbitals is lifted as the molecule bends. The molecular orbital corresponding to the p orbital in the molecular plane becomes bonding and correlates with the $3a_1$ molecular orbital of the bent molecule. The other molecular orbital, which is perpendicular to the molecular plane, remains a nonbonding orbital and correlates with the $1b_1$ orbital of the bent molecule. The angle dependence of the $1\pi_u - 3a_1$ orbital energy is of particular importance, because this orbital is the only one that becomes signif-

icantly more stable in the nonlinear geometry. All other molecular orbitals are destabilized when the HAH angle is decreased. The occupation of this orbital with one or two electrons can result in a bent equilibrium structure of the molecule. Correlation diagrams as the one shown in Figure 5.8 are known as Walsh diagrams.

As in the case of atoms and diatomic molecules, the electronic configurations of polyatomic molecules are obtained by filling the molecular orbitals with a maximum of two electrons. Whether a molecule of the form HAH is linear or bent depends on the occupation of the orbitals, especially of the $3a_1$ orbital, as discussed above. The symmetries of the electronic states that result from a given configuration are obtained from the direct product of the irreducible representations of the occupied molecular orbitals (see Section 4.3.4). Finally, the multiplicities $(2S + 1)$ are derived following exactly the same procedure as discussed for atoms and diatomic molecules in chapters 2 and 3 (see also Section 5.1.4 below).

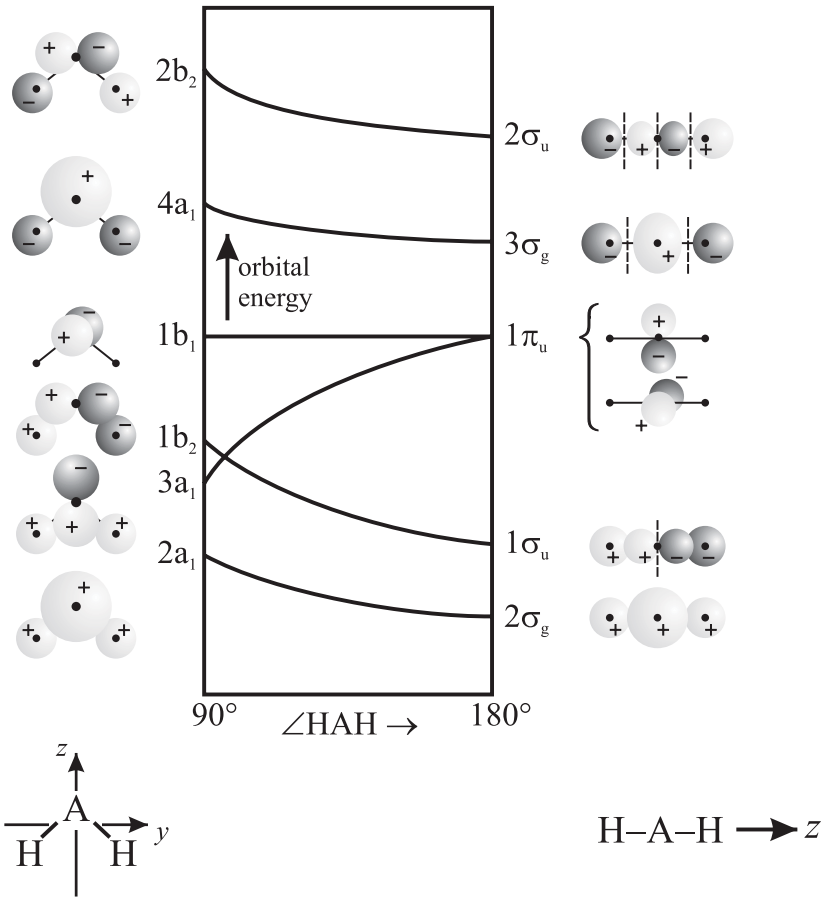

Figure 5.8: Walsh diagram for HAH molecules. The symmetry labels on the left-hand side correspond to C_{2v} point-group symmetry, those on the right-hand side to $D_{\infty h}$ symmetry.

Examples:

BeH_2: $\ldots(2\sigma_g)^2(1\sigma_u)^2$

The dependence of the energies of the occupied orbitals favors a linear structure (see Figure 5.8) and the ground electronic state is therefore the $\tilde{X}\ ^1\Sigma_g^+$ state.

BeH_2: $\ldots(2a_1)^2(1b_2)^1(3a_1)^1$

The first excited configuration leads to a bent structure because the $3a_1 - 1\pi_u$ orbital is occupied. The electronic configuration is thus given using C_{2v} symmetry labels. The two electronic states resulting from this configuration are of $^3B_2$ and $^1B_2$ symmetry.

H_2O: $\ldots(2a_1)^2(1b_2)^2(3a_1)^2(1b_1)^2$

Because the $3a_1$ orbital in H_2O is doubly occupied, the electronic ground state is also bent. The ground electronic state is thus the $\tilde{X}\ ^1A_1$ state.

H_2O^+: $\ldots(2a_1)^2(1b_2)^1(3a_1)^2(1b_1)^1$ $\tilde{X}^+\ ^2B_1$.

Walsh diagrams such as that displayed in Figure 5.8 are also useful in the discussion of vibronic interactions because they enable one to see how the degeneracy of π orbitals and of the $\Pi, \Delta, \Phi, \ldots$ electronic states are lifted, and how the electronic character changes, when the molecules bend out of their linear structures.

Larger symmetric molecules

To determine the molecular orbitals of larger polyatomic molecules that have a high symmetry, it is useful to follow the systematic approach introduced in chapter 4; the symmetrized linear combination of atomic orbitals (LCAO) are determined using projection operators $\hat{P}^{\Gamma}$ (Equation (4.11)) that are applied onto one of the atomic orbitals of the set of identical atoms.

To illustrate the application of the projection formula, we use it to derive the system of π molecular orbitals of benzene in the D_{6h} point group by building symmetry-adapted linear combinations

$$\Phi_{\Gamma}^{(s)} = \sum_{i=1}^{6} c_{\Gamma,i}\, \phi_i \tag{5.40}$$

of the carbon $2p_z$ orbitals φ_i $(i = 1 - 6)$. From the six $2p_z$ atomic orbitals involved in the π orbital system, which form a six-dimensional reducible representation of the D_{6h} point group, a total of 6 orthogonal molecular orbitals can be formed. The reducible representation Γ of the carbon $2p_z$ orbitals can be constructed using the character table of the D_{6h} point group presented in Table 5.2.

Under the group operations of D_{6h}, the $2p_z$ orbitals φ_i have the same symmetry properties as the components z_i of the nuclear displacement vectors of the carbon atoms. The $2p_z$ orbitals are mapped onto each other by the symmetry operations of the group. From the properties of the representation matrices, it can be easily established that

- each orbital that is left unchanged by a symmetry operation $\hat{O}$ adds 1 to the character $\chi(\hat{O})$,
- each orbital that is inverted adds -1 to the character,
- each orbital that is mapped onto another orbital gives no contribution to the character.

D_{6h}	E	$2C_6$	$2C_3$	C_2	$3C_2'$	$3C_2''$	i	$2S_3$	$2S_6$	σ_h	$3\sigma_d$	$3\sigma_v$	
A_{1g}	1	1	1	1	1	1	1	1	1	1	1	1	
A_{2g}	1	1	1	1	-1	-1	1	1	1	1	-1	-1	R_z
B_{1g}	1	-1	1	-1	1	-1	1	-1	1	-1	1	-1	
B_{2g}	1	-1	1	-1	-1	1	1	-1	1	-1	-1	1	
E_{1g}	2	1	-1	-2	0	0	2	1	-1	-2	0	0	R_x, R_y
E_{2g}	2	-1	-1	2	0	0	2	-1	-1	2	0	0	
A_{1u}	1	1	1	1	1	1	-1	-1	-1	-1	-1	-1	
A_{2u}	1	1	1	1	-1	-1	-1	-1	-1	-1	1	1	z
B_{1u}	1	-1	1	-1	1	-1	-1	1	-1	1	-1	1	
B_{2u}	1	-1	1	-1	-1	1	-1	1	-1	1	1	-1	
E_{1u}	2	1	-1	-2	0	0	-2	-1	1	2	0	0	x, y
E_{2u}	2	-1	-1	2	0	0	-2	1	1	-2	0	0	

Table 5.2: Character table of the D_{6h} point group.

Thus, the characters of the reducible representation Γ of the six $2p_z$ orbitals under the different classes of symmetry operations $\hat{O}$ are

D_{6h}	E	$2C_6$	$2C_3$	C_2	$3C_2'$	$3C_2''$	i	$2S_3$	$2S_6$	σ_h	$3\sigma_d$	$3\sigma_v$
Γ	6	0	0	0	-2	0	0	0	0	-6	0	2

Reducing Γ using Equation (4.10) yields the symmetries of the six π molecular orbitals:

$$\Gamma = B_{2g} \oplus A_{2u} \oplus E_{1g} \oplus E_{2u}, \tag{5.41}$$

each of the two e irreducible representations being two-dimensional. The orthonormal set of symmetry-adapted basis functions $\{\Phi_i^{(s)}\}$ is constructed by projecting the φ_i on their irreducible components using Equation (4.11) (projection operator) and Table 5.2:

$$\Phi_{A_{2u}}^{(s)} = \frac{1}{N}\hat{P}^{A_{2u}}\phi_1 = \frac{1}{\sqrt{6}}\big(\phi_1 + \phi_2 + \phi_3 + \phi_4 + \phi_5 + \phi_6\big), \tag{5.42}$$

where N is a normalization constant. The same result is obtained by applying the projector to any other $\phi_i,\ i \neq 1$.

$$\Phi_{B_{2g}}^{(s)} = \frac{1}{N}\hat{P}^{B_{2g}}\phi_1 = \frac{1}{\sqrt{6}}\big(\phi_1 - \phi_2 + \phi_3 - \phi_4 + \phi_5 - \phi_6\big). \tag{5.43}$$

For multi-dimensional subspaces, the projection technique usually yields nonorthogonal linear combinations of the original basis vectors. To construct the symmetry-adapted basis, it is sufficient to determine d_i linearly independent vectors and then choose suitable orthogonal linear combinations of them:

$$\Phi^{(\mathrm{s})}_{\mathrm{E_{1g}},1} = \frac{1}{N}\hat{P}^{\mathrm{E_{1g}}}\phi_1 = \frac{1}{\sqrt{12}}\big(2\phi_1 + \phi_2 - \phi_3 - 2\phi_4 - \phi_5 + \phi_6\big), \tag{5.44}$$

$$\Phi^{(\mathrm{s})}_{\mathrm{E_{1g}},2} = \frac{1}{N}\hat{P}^{\mathrm{E_{1g}}}\phi_2 = \frac{1}{\sqrt{12}}\big(\phi_1 + 2\phi_2 + \phi_3 - \phi_4 - 2\phi_5 - \phi_6\big). \tag{5.45}$$

The set of vectors $\{\Phi^{(\mathrm{s})}_{\mathrm{E_{1g}},1}, \Phi^{(\mathrm{s})}_{\mathrm{E_{1g}},2}\}$ is linearly independent, but not orthogonal. A set of orthogonal basis vectors can be obtained by using the Schmidt orthogonalization algorithm: if ψ_1, ψ_2 are non-orthogonal, normalized basis vectors, then a basis vector $\psi_2^{\perp}$ which is orthogonal to ψ_1 can be constructed using Equation (5.46):

$$\psi_2^{\perp} = \psi_2 - \big\langle\psi_2\big|\psi_1\big\rangle\psi_1, \tag{5.46}$$

where $\langle .|. \rangle$ denotes the scalar product. Thus:

$$\begin{aligned}\Phi^{(\mathrm{s}),\perp}_{\mathrm{E_{1g}},2} &= \Phi^{(\mathrm{s})}_{\mathrm{E_{1g}},2} - \big\langle\,\Phi^{(\mathrm{s})}_{\mathrm{E_{1g}},2}\big|\,\Phi^{(\mathrm{s})}_{\mathrm{E_{1g}},1}\big\rangle\,\Phi^{(\mathrm{s})}_{\mathrm{E_{1g}},1} \\ &= \Phi^{(\mathrm{s})}_{\mathrm{E_{1g}},2} - \frac{1}{2}\Phi^{(\mathrm{s})}_{\mathrm{E_{1g}},1}.\end{aligned} \tag{5.47}$$

After normalization, one obtains

$$\Phi^{(\mathrm{s}),\perp}_{\mathrm{E_{1g}},2} = \frac{1}{2}\big(\phi_2 + \phi_3 - \phi_5 - \phi_6\big). \tag{5.48}$$

The set of symmetry-adapted basis vectors $\{\Phi^{(\mathrm{s})}_{\mathrm{E_{1g,a}}}, \Phi^{(\mathrm{s})}_{\mathrm{E_{1g,b}}}\} = \{\Phi^{(\mathrm{s})}_{\mathrm{E_{1g}},1}, \Phi^{(\mathrm{s}),\perp}_{\mathrm{E_{1g}},2}\}$ for the $\mathrm{E_{1g}}$ subspace is thus:

$$\Phi^{(\mathrm{s})}_{\mathrm{E_{1g,a}}} = \frac{1}{\sqrt{12}}\big(2\phi_1 + \phi_2 - \phi_3 - 2\phi_4 - \phi_5 + \phi_6\big), \tag{5.49}$$

$$\Phi^{(\mathrm{s})}_{\mathrm{E_{1g,b}}} = \frac{1}{2}\big(\phi_2 + \phi_3 - \phi_5 - \phi_6\big). \tag{5.50}$$

Similarly, one obtains an orthonormal set of symmetry-adapted basis vectors for the $\mathrm{E_{2u}}$ subspace:

$$\Phi^{(\mathrm{s})}_{\mathrm{E_{2u,a}}} = \frac{1}{\sqrt{12}}\big(2\phi_1 - \phi_2 - \phi_3 + 2\phi_4 - \phi_5 - \phi_6\big), \tag{5.51}$$

$$\Phi^{(\mathrm{s})}_{\mathrm{E_{2u,b}}} = \frac{1}{2}\big(\phi_2 - \phi_3 + \phi_5 - \phi_6\big). \tag{5.52}$$

These molecular orbitals are depicted in Figure 5.9. Their energetic ordering can be determined from the number of nodal planes. The $\mathrm{a_{2u}}$ orbital must be the most stable because

it possesses a single nodal plane (the plane containing the carbon atoms). The e_{1g} orbital possesses two nodal planes and has therefore the second lowest energy. The e_{2u} and b_{2g} orbitals possess three and four nodal planes and are thus the orbitals of second highest and highest energy, respectively.

A more quantitative estimate of the relative energies of the molecular orbitals can be achieved using the Hückel molecular orbital (HMO) model. The HMO model represents a simple semi-empirical method to calculate the electronic energy level structure of molecules that exhibit conjugated π molecular orbitals such as polyenes and aromatic molecules. The model is useful to gain a semi-quantitative description of the π molecular orbitals and their relative energies and is widely used in physical-organic chemistry. Within the framework of the HMO model, the π molecular orbitals are constructed by linear combinations of orthogonal $2p_z$ atomic orbitals centered on the carbon atoms. The energies E_k of the π molecular orbitals are obtained by solving the secular determinant

$$\det(H_{ij} - E_k S_{ij}) = 0, \tag{5.53}$$

where H_{ij} are the matrix elements of a formal Hamiltonian operator $\hat{H}$ describing the π electron system (the "Hückel operator") and S_{ij} denotes the overlap integral between the p_z orbitals of atoms i and j. The expansion coefficients $c_i^{(k)}$ of the molecular orbital Φ_k in the basis of the atomic $2p_z$ orbitals $\{\varphi_i\}$ are obtained by solving the set of secular equations

$$\sum_i c_i^{(k)} \big(H_{ij} - E_k S_{ij}\big) = 0. \tag{5.54}$$

The following approximations are introduced:

- All overlap integrals vanish ($S_{ij} = 0$) unless $i = j$, in which case $S_{ii} = 1$.
- All diagonal elements of $\boldsymbol{H}$ are the same: $H_{ii} = \alpha$.
- All off-diagonal elements of $\boldsymbol{H}$ are set to zero, except those between neighboring atoms, which are $H_{ij} = \beta$. β is usually negative ($\beta < 0$).

α and β are treated as effective parameters that can in principle be estimated from calorimetric data.

The matrix representation of the Hückel operator $\hat{H}$ describing the π molecular orbital system

can be derived in the basis of the carbon $2p_z$ atomic orbitals $\{\phi_i\}$, and is

$$\boldsymbol{H} = \begin{bmatrix} \alpha & \beta & 0 & 0 & 0 & \beta \\ \beta & \alpha & \beta & 0 & 0 & 0 \\ 0 & \beta & \alpha & \beta & 0 & 0 \\ 0 & 0 & \beta & \alpha & \beta & 0 \\ 0 & 0 & 0 & \beta & \alpha & \beta \\ \beta & 0 & 0 & 0 & \beta & \alpha \end{bmatrix}. \tag{5.55}$$

The eigenvectors and eigenvalues of the matrix (5.55) represent the molecular orbitals and their energies, respectively. Alternatively, the Hückel operator can be expressed in the basis of symmetry-adapted basis function $\{\Phi_i^{(s)}\}$ by evaluating the matrix elements according to

$$H_{ij}^{(s)} = \langle \Phi_i^{(s)} | \hat{H} | \Phi_j^{(s)} \rangle \tag{5.56}$$

using the basis functions given in Equations (5.42), (5.43), (5.49), (5.50), (5.51), (5.52). For the $\Phi_{A_{2u}}^{(s)}$ orbital (Equation (5.42)), one finds, for instance:

$$\begin{aligned} \langle \Phi_{A_{2u}}^{(s)} | \hat{H} | \Phi_{A_{2u}}^{(s)} \rangle &= \frac{1}{6} \langle \phi_1 + \phi_2 + \phi_3 + \phi_4 + \phi_5 + \phi_6 | \hat{H} | \phi_1 + \phi_2 + \phi_3 + \phi_4 + \phi_5 + \phi_6 \rangle \\ &= \alpha + 2\beta. \end{aligned} \tag{5.57}$$

Matrix elements between functions of different symmetry and matrix elements between orthogonal basis functions within the E_{1g} and E_{2u} subspaces are zero because $\boldsymbol{H}$ is totally symmetric, so that one obtains the following Hückel matrix

$$\boldsymbol{H}^{(s)} = \begin{bmatrix} \alpha + 2\beta & 0 & 0 & 0 & 0 & 0 \\ 0 & \alpha - 2\beta & 0 & 0 & 0 & 0 \\ 0 & 0 & \alpha + \beta & 0 & 0 & 0 \\ 0 & 0 & 0 & \alpha + \beta & 0 & 0 \\ 0 & 0 & 0 & 0 & \alpha - \beta & 0 \\ 0 & 0 & 0 & 0 & 0 & \alpha - \beta \end{bmatrix}, \tag{5.58}$$

which is already in diagonal form. The symmetry-adapted orthonormal basis functions $\{\Phi_i^{(s)}\}$ are thus the eigenvectors of the Hückel operator and represent the π molecular orbitals of benzene depicted in Figure 5.9.

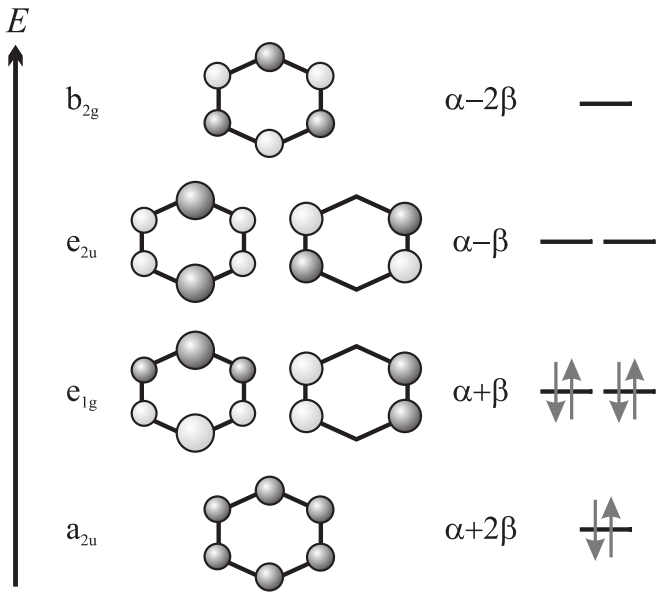

Figure 5.9: Energy level diagram and schematic representation of the π molecular orbitals of benzene. The size of the circles represents the weight of the atomic orbital in the molecular orbital wave function. The two grey tones of the shading indicate the relative sign of the $2p_z$ orbitals which form the molecular orbital. The energies of the molecular orbitals increase with the number of nodal planes and are expressed, on the right-hand side of the figure, as a function of the Hückel parameters α and β. The arrows represent schematically the occupation of the molecular orbitals in the ground-state configuration of benzene.

One should note that a group theoretical treatment normally only divides the Hamiltonian matrix in as many diagonal blocks as there are irreducible representations, *i. e.*, in the present case, in two 1×1 diagonal blocks corresponding to A_{2u} and A_{2g} and two 2×2 diagonal blocks corresponding to E_{1g} and E_{2u}. The fact that the Hamiltonian matrix is fully diagonal in Equation (5.58) is a consequence of the particular choice made during the Schmidt orthogonalization procedure.

The lowest energy configuration of π electrons in benzene can thus be written $(a_{2u})^2(e_{1g})^4$, giving rise to a single electronic state of symmetry $^1A_{1g}$. The first excited electronic configuration of benzene is $(a_{2u})^2(e_{1g})^3(e_{2u})^1$. This configuration gives rise to several electronic states as will be discussed in Section 5.1.4. The direct product of the partially occupied orbitals is $E_{1g} \otimes E_{2u} = B_{1u} \oplus B_{2u} \oplus E_{1u}$. Since two different spatial orbitals are partially occupied, there is no restriction on the total electron spin imposed by the generalized Pauli principle (see Section 3.4.3), and all electronic states contained in the direct product can exist

as either singlet or triplet states. The configuration $(a_{2u})^2(e_{1g})^3(e_{2u})^1$ thus gives rise to the electronic states $^3B_{1u}$, $^1B_{1u}$, $^3B_{2u}$, $^1B_{2u}$, $^3E_{1u}$ and $^1E_{1u}$.

To illustrate the case where each orbital of a degenerate pair of orbitals is singly occupied, we now present the group theoretical and HMO treatments of the electronic structure of the cyclopentadienyl cation $C_5H_5^+$ using the D_{5h} point group, the character table of which is presented in Table 5.3.

D_{5h}	E	$2C_5$	$2C_5^2$	$5C_2$	σ_h	$2S_5$	$2S_5^2$	$5\sigma_d$	
A_1'	1	1	1	1	1	1	1	1	
A_2'	1	1	1	-1	1	1	1	-1	R_z
E_1'	2	ω_2	ω_1	0	2	ω_2	ω_1	0	x, y
E_2'	2	ω_1	ω_2	0	2	ω_1	ω_2	0	
A_1''	1	1	1	1	-1	-1	-1	-1	
A_2''	1	1	1	-1	-1	-1	-1	1	z
E_1''	2	ω_2	ω_1	0	-2	$-\omega_2$	$-\omega_1$	0	R_x, R_y
E_2''	2	ω_1	ω_2	0	-2	$-\omega_1$	$-\omega_2$	0	

Table 5.3: Character table of the D_{5h} point group with ω_1=2 cos(4π/5) and ω_2=2 cos(2π/5).

The matrix representation of the Hückel operator can be determined in analogy to benzene and takes the form

$$\boldsymbol{H} = \begin{bmatrix} \alpha & \beta & 0 & 0 & \beta \\ \beta & \alpha & \beta & 0 & 0 \\ 0 & \beta & \alpha & \beta & 0 \\ 0 & 0 & \beta & \alpha & \beta \\ \beta & 0 & 0 & \beta & \alpha \end{bmatrix} . \tag{5.59}$$

Diagonalization of this matrix gives rise to the five eigenvalues $\alpha + 2\beta$, $\alpha + \omega_1\beta$ and $\alpha + \omega_2\beta$, where ω_1 and ω_2 are defined in Table 5.3. The application of the reduction formula of Equation (4.10) to the five-dimensional reducible representation of the five p_z orbitals and of the projection operators gives rise to five eigenvectors of symmetries A_2'', E_1'' and E_2''. The energetic ordering of the corresponding orbitals is depicted in Figure 5.10a in the form of a so-called Frost-Musulin diagram. A Frost-Musulin diagram is derived by drawing a regular

polygone representing the cyclic polyene into a circle, placing one vertex on the lowest point of the circle. The vertices of the polygone then provide the energies of the π orbitals of the polyene. Such diagrams provide an elegant graphical method to determine the sequence and degeneracy of the HMO of cyclic polyenes. Looking back at Figure 5.9, it becomes apparent that a Frost-Musulin diagram indeed adequately describes the HMOs of benzene.

The most stable electronic configuration of $C_5H_5^+$ is $(a_2'')^2(e_1'')^2$, as depicted in Figure 5.10a. The direct product of the irreducible representations of the partially occupied orbitals is $E_1'' \otimes E_1'' = A_2' \oplus E_2' \oplus A_1'$. In this case, the two components of a degenerate orbital may both be singly occupied. The total electronic wave function must be antisymmetric under the exchange of the two electrons in the e_1'' orbitals, which restricts the number of possible states, as will be discussed in general terms in Section 5.1.4. The singlet states have an antisymmetric electron spin wave function (with respect to the permutation of the electrons). By consequence, this electron spin wave function must be combined with the *symmetric* (rather than the *direct*) product of the irreducible representations $[E_1'' \otimes E_1''] = E_2' \oplus A_1'$, resulting in a $^1E_2'$ and a $^1A_1'$ state. Correspondingly, the triplet state has a symmetric electron spin wave function (with respect to the permutation of the electrons). By consequence, this electron spin wave function must be combined with the antisymmetric product $\{E_1'' \otimes E_1''\} = A_2'$, resulting in a single $^3A_2'$ state (see the analogous discussion of the electronic structure of O_2 in Subsection 3.4.3). The energetic ordering of the three states $^3A_2'$, $^1E_2'$ and $^1A_1'$ is given in Figure 5.10b. The Hartree-Fock energies of these three states are $2h + J_{23} - K_{23}$, $2h + J_{23} + K_{23}$ and $2h + J_{22} + K_{23}$, respectively, where h, J_{ij} and K_{ij} represent the one-electron orbital energy, the Coulomb and the exchange integrals, respectively, and the indices designate the π molecular orbitals in order of increasing energy (by symmetry, $J_{22} - J_{23} = 2K_{23}$, see *e. g.* W. T. Borden, *Diradicals*, John Wiley and Sons, New York (1982)). Using the Hückel molecular orbital approach, one can determine the one-electron energy to be $h = \alpha + \omega_1\beta$.

Large polyatomic molecules

Unlike small polyatomic molecules, most large molecules have a low symmetry, and the classification of electronic states by their irreducible representations loses its relevance. When the molecule possesses no symmetry elements, all electronic transitions involving nominally a single electron are allowed by symmetry. Consequently, a different nomenclature is used to label both the electronic states and the electronic transitions of large molecules, as already mentioned in the introduction.

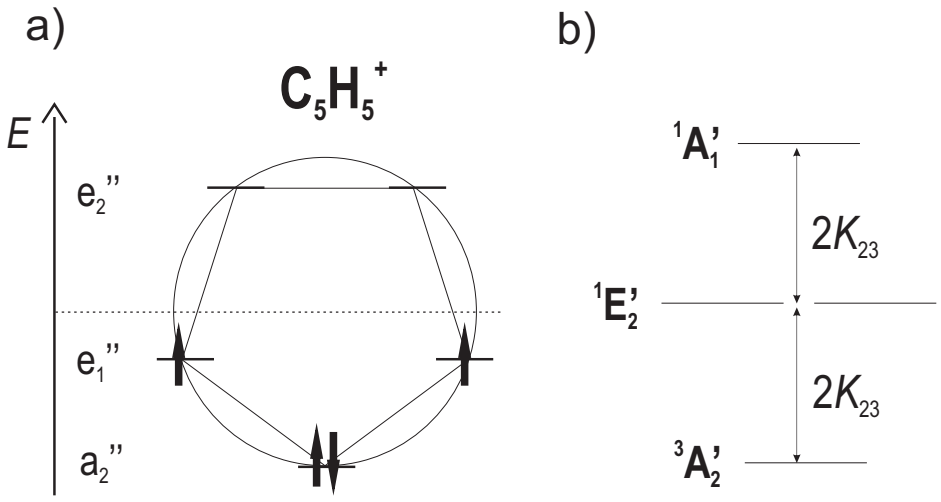

Figure 5.10: a) Frost-Musulin diagram of the π molecular orbitals of the cyclopentadienyl cation. The arrows indicate the occupation corresponding to the lowest-lying electronic configuration. b) Energetic ordering of the corresponding electronic states in D_{5h} symmetry (right-hand side). K_{23} represents the exchange integral (adapted from H. J. Wörner and F. Merkt, *J. Chem. Phys.*, **127**, 034303 (2007)).

The electronic states are designated by a capital letter representing their spin multiplicity: S for singlets, D for doublets, T for triplets etc. A numerical subscript is used to indicate the ground state (*e. g.* S_0) and the higher-lying excited states of the same multiplicity (S_1, S_2 etc...). States of another multiplicity of the same molecule are also labelled in order of increasing energies but starting with the subscript "1" rather than "0" (*e. g.* T_1, T_2 etc.).
Electronic transitions in polyatomic molecules are often labeled according to the type of molecular orbitals involved. One distinguishes between bonding orbitals of σ or π type, the corresponding anti-bonding orbitals (σ^* or π^*) and nonbonding orbitals (n). This nomenclature has the advantage that it highlights the nature of the electronic transition, from which qualitative predictions of their intensities can be made: Transitions involving the excitation of an electron from a bonding to the corresponding antibonding orbital ($\sigma \rightarrow \sigma^*$ or $\pi \rightarrow \pi^*$) are usually associated with a large oscillator strength, whereas transitions from nonbonding to anti-bonding orbitals ($n \rightarrow \sigma^*$ or $n \rightarrow \pi^*$) are weak.
The nomenclature outlined above is often used in the discussion of the photochemistry and photophysics of larger molecules, like the DNA bases. Although the isolated DNA bases absorb strongly in the ultraviolet (200-300 nm), they hardly show any fragmentation, unlike many other molecules. This property may be of importance in preserving the genetic infor-

mation (see *e. g.* A. L. Sobolewski and W. Domcke, *Eur. Phys. J. D*, 20, 369–374 (2002).) and arises from the ability of the molecules to convert the energy of the photon to vibrational energy.

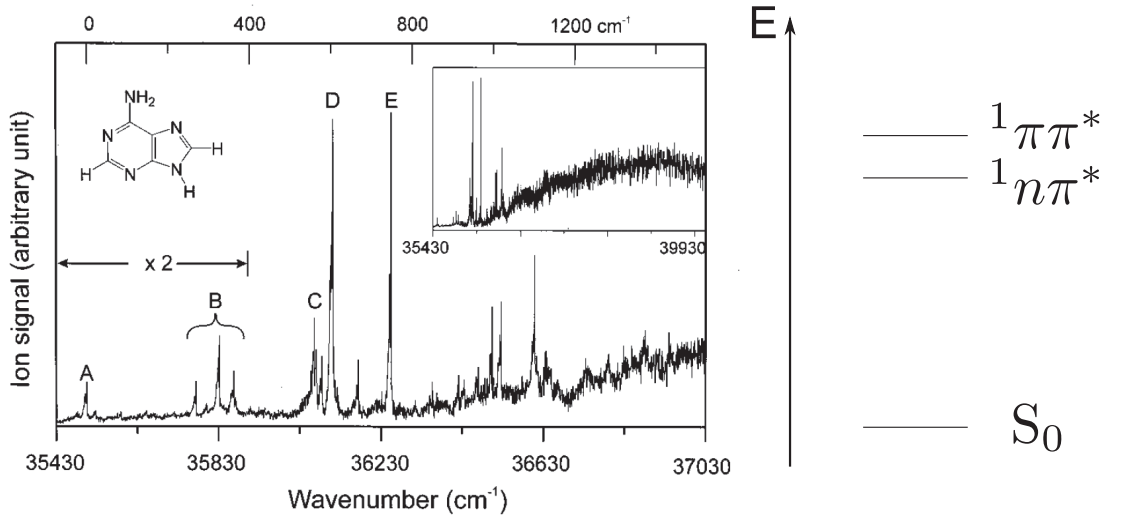

Figure 5.11: Resonance-enhanced two-photon ionization spectrum of adenine in the gas phase (adapted from N. J. Kim *et al.*, *J. Chem. Phys.*, **113**, 10051–10055 (2000)). The bands A and D are assigned to the origins of the $n \rightarrow \pi^*$ and $\pi \rightarrow \pi^*$ excitations, respectively. The bands B, C and E are vibronic levels of mixed electronic character. The right-hand side of the figure shows an energy level diagram of the three lowest electronic singlet states of adenine.

Adenine also represents a good example illustrating the difficulty associated with all nomenclature systems for large molecules. The sequence of singlet states consists of the S_0 ground state with the configuration $\ldots(\pi)^2(n)^2(\pi^*)^0$, followed by two electronic states of dominant configurations, $\ldots(\pi)^2(n)^1(\pi^*)^1$ and $\ldots(\pi)^1(n)^2(\pi^*)^1$, respectively. One can only indicate the dominant configurations for these two electronic states because they lie energetically very close, and configuration interaction between them is important. Since the energetic ordering of these states has been debated in the literature, it is difficult to apply the usual labels S_1 and S_2 to these electronic states. To avoid this difficulty, the recent literature uses the designation $^1n\pi^*$ and $^1\pi\pi^*$ for these two states, the ^{1} superscript designating the spin multiplicity. Figure 5.11 shows a resonant two-photon ionization spectrum of adenine in a supersonic expansion and a diagram of the electronic energy levels as derived from the spectrum. The band labeled "A" was assigned to the origin of the $^1n\pi^*$ state, whereas band "D" was assigned to the origin of the $^1\pi\pi^*$ state. The wave number scale on top of Figure 5.11 is given with respect to band "A". The energy-integrated absorption of the $^1\pi\pi^*$ state is strong, and the

band turns into a broad absorption band above 36230 cm^{-1}.

5.1.4 Spin multiplicity

As in the treatment of diatomic molecules in Subsection 3.4.3, we will only consider two-electron wave functions. Because of the Pauli principle, the two-electron wave function must either have a symmetric spatial part ($\Psi^{\mathrm{R}}_{(\mathrm{s})}(q_i)$) and an antisymmetric spin part ($\Psi^{\mathrm{S}}_{(\mathrm{a})}(m_i)$) or vice versa ($\Psi^{\mathrm{R}}_{(\mathrm{a})}(q_i)$) and ($\Psi^{\mathrm{S}}_{(\mathrm{a})}(m_i)$), see Tables 2.2 and 2.3.
The situation is slightly different from the case of diatomic molecules, because the components of degenerate orbitals can no longer be classified according to a good quantum number (λ in the case of diatomic molecules). However, group theory provides a simple approach to determining the existing multiplicities. Two cases can be distinguished:

1. The two electrons are located in different molecular-orbital shells. Both the symmetric and the antisymmetric spatial parts of the wave functions are nonzero in this case. No restrictions result from the Pauli principle: The electronic states are given by the direct product of the representations of the partially occupied orbitals, and all terms contained in the direct product exist as both singlet and triplet states. This situation arises in the first excited states of BeH_2 arising from the configuration $\ldots(2a_1)^2(1b_2)^1(3a_1)^1$. Since $b_2 \otimes a_1 = b_2$, the two electronic states $^3B_2$ and $^1B_2$ are obtained. The same applies to the $(a_{2u})^2(e_{1g})^3(e_{2u})^1$ configuration of benzene discussed in Section 5.1.3b, giving rise to the electronic states $^3B_{1u}$, $^1B_{1u}$, $^3B_{2u}$, $^1B_{2u}$, $^3E_{1u}$ and $^1E_{1u}$.

2. The two electrons are located in the same molecular-orbital shell. If the molecular-orbital shell is nondegenerate, the spatial part of the wave function is necessarily symmetric. The spin part must therefore be antisymmetric, resulting in a totally symmetric (A'_1) singlet state. If the molecular-orbital shell is degenerate, the spatial part has both symmetric and anti-symmetric components. The symmetry properties of these components is determined by the symmetric and antisymmetric parts, respectively, of the direct product of the orbital symmetry with itself. This situation arises in the $(a''_2)^2(e''_1)^2$ configuration of $C_5H_5^+$ discussed in Section 5.1.3b. The symmetric spatial part of the wave function is given by $[E''_1 \otimes E''_1] = E'_2 \oplus A'_1$, resulting in a $^1E'_2$ and a $^1A'_1$ state. Correspondingly, the triplet state is obtained from the antisymmetric product $\{E''_1 \otimes E''_1\} = A'_2$, resulting in a single $^3A'_2$ state.

5.2 Spectra of polyatomic molecules

5.2.1 Rovibrational Transitions

As discussed in Section 4.3.6, a vibrational transition is allowed when the matrix element $\langle \phi'_{\rm vib}\phi''_{\rm el}|\mu_\alpha|\phi''_{\rm el}\phi''_{\rm vib}\rangle$ is non-zero, *i. e.* when the irreducible representations of the vibrational levels and the dipole operator fulfill the following relation

$$\Gamma'_{\rm vib} \otimes \Gamma_\alpha \otimes \Gamma''_{\rm vib} \ni {\rm A}_1. \tag{5.60}$$

When vibrational transitions are measured at high resolution, they reveal their rotational structure which follows the following selection rules:

- symmetric tops:
  $\alpha = z$, parallel transition, $\Delta K = 0$, $\Delta J = \pm 1$ for $K = 0$ and $\Delta J = 0, \pm 1$ for $K \neq 0$.
  $\alpha = x, y$, perpendicular transition, $\Delta K = \pm 1$, $\Delta J = 0, \pm 1$.

- asymmetric tops:
  $\alpha = a$, "a-type" transition, ΔK_a even, ΔK_c odd, $\Delta J = \pm 1$ for $K_a = 0$
  and $\Delta J = 0, \pm 1$ for $K_a \neq 0$.
  $\alpha = b$, "b-type" transition, ΔK_a odd, ΔK_c odd, $\Delta J = \pm 1$.
  $\alpha = c$, "c-type" transition, ΔK_a odd, ΔK_c even, $\Delta J = \pm 1$ for $K_c = 0$
  and $\Delta J = 0, \pm 1$ for $K_c \neq 0$.

Figure 5.12 shows a high-resolution Fourier-transform infrared spectrum of the ν_1 fundamental band of CHD_2I, which is an asymmetric top. The panel in the center shows an overview of the spectrum in which both a- and c-type transitions are visible. The top panel shows an enlarged view of the low-wavenumber-side of the spectrum in which c-type transitions with $\Delta K_{\rm a} = -1$ dominate. The bottom panel shows an enlarged view of the region in which a-type transitions with $\Delta J = +1$ dominate (R-branch).

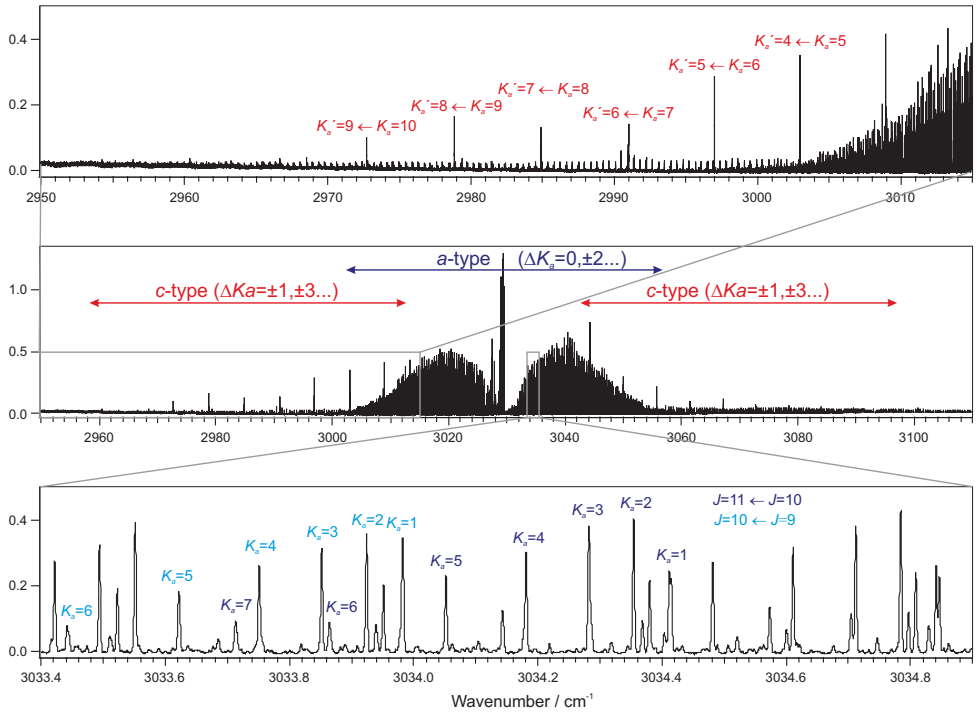

Figure 5.12: Fourier transform infrared spectrum of the ν_1 fundamental of CHD_2I (data from S. Albert, C. Manca Tanner, and M. Quack, *Molecular Physics*, *108*, 2403-2426 (2010)).

5.2.2 Electronic Transitions

An electronic transition is allowed if the matrix element $\langle\phi'_{\rm el}|\mu_\alpha|\phi''_{\rm el}\rangle$ is non-zero, *i. e.* when the irreducible representations of the electronic states and the dipole operator fulfill the following relation

$$\Gamma'_{\rm el} \otimes \Gamma_\alpha \otimes \Gamma''_{\rm el} \ni {\rm A}_1. \tag{5.61}$$

When an electronic transition is allowed, the vibrational structure of the transition can be predicted by factorizing the matrix element

$$\langle\phi'_{\rm vib}\phi'_{\rm el}|\mu_\alpha|\phi''_{\rm el}\phi''_{\rm vib}\rangle = \langle\phi'_{\rm vib}|\phi''_{\rm vib}\rangle\langle\phi'_{\rm el}|\mu_\alpha|\phi''_{\rm el}\rangle. \tag{5.62}$$

Consequently, a transition to a final vibrational state $\phi'_{\rm vib}$ will only be observable if the irreducible representations of the two vibrational states fulfil the relation:

$$\Gamma'_{\rm vib} \otimes \Gamma''_{\rm vib} \ni {\rm A}_1. \tag{5.63}$$

Just as in diatomic molecules, the quantity $|\langle\phi'_{\rm vib}|\phi''_{\rm vib}\rangle|^2$ determines the relative intensities of the vibrational bands in an electronic transition and is called the "Franck-Condon factor" (see

Chapter 3 and Figure 3.12).

When an electronic transition is forbidden, it can sometimes nevertheless be weakly observed through coupling of the electronic and vibrational degrees of freedom. The mechanism by which such transitions are observed is the Herzberg-Teller intensity borrowing mechanism mentioned in the section entitled "Electronically forbidden but vibronically allowed transitions". Since the electronic wave functions depend parametrically on the nuclear coordinates Q, the factorization used in Equation (5.62) is not adequate when the electronic wave functions change significantly with the molecular geometry. This is however often the case when electronic states are close to each other and especially for molecular geometries deviating from the highest symmetry. In such cases, electronically forbidden transitions can become observable if the following relation is fulfilled:

$$\Gamma'_{\mathrm{vib}} \otimes \Gamma'_{\mathrm{el}} \otimes \Gamma_{\alpha} \otimes \Gamma''_{\mathrm{el}} \otimes \Gamma''_{\mathrm{vib}} \ni \mathrm{A}_1. \tag{5.64}$$

Example: Let us consider the electronically forbidden transition between the $\tilde{\mathrm{X}}\ ^1\mathrm{A}_1$ vibrationless ground state and the $\tilde{\mathrm{Y}}\ ^1\mathrm{A}_2$ electronic state of a $C_{2\mathrm{v}}$ molecule. Excitation of a B_1 vibration in the upper electronic state results in an excited state of vibronic symmetry $\Gamma_{\mathrm{ev}} = \mathrm{A}_2 \otimes \mathrm{B}_1 = \mathrm{B}_2$. A transition to this state originating in the A_1 state is vibronically allowed. However, the transition only carries significant intensity if the B_2 vibronic state interacts with a close-lying electronic state $\tilde{\mathrm{Z}}$ of electronic symmetry B_2. The intensity of the transition is 'borrowed' from the $\tilde{\mathrm{Z}} \leftarrow \tilde{\mathrm{X}}$ by the Herzberg-Teller effect.

Electronically allowed transitions

In polyatomic molecules, an electronic transition can be induced by any of the three Cartesian components of the transition dipole moment. When an electronic transition is allowed, the relative intensities of the transitions to different vibrational levels of the electronically excited state approximately correspond to Franck-Condon factors, and the vibrational structure of an electronically allowed transition contains information on the relative equilibrium geometries of the two electronic states connected through the transition.

An illustrative example of an electronically allowed transition is the absorption spectrum of ammonia, which is displayed in Figure 5.13. The electronic ground state of ammonia has an equilibrium structure of pyramidal $C_{3\mathrm{v}}$ point-group symmetry. However, two pyramidal

configurations are separated by a low barrier along the symmetric bending (umbrella) mode, which leads to inversion of the molecule through tunneling on the picosecond time scale and to a tunneling splitting of $0.8\,\mathrm{cm}^{-1}$. When this tunneling splitting is resolved, the appropriate point group to treat the energy level structure is $D_{3\mathrm{h}}$, the character table of which is given in Table 5.4.

$\mathrm{D_{3h}}$	I	$2\mathrm{C}_3$	$3\mathrm{C}_2$	σ_h	$2\mathrm{S}_3$	$3\sigma_\mathrm{v}$	
A_1'	1	1	1	1	1	1	
A_2'	1	1	−1	1	1	−1	R_z
E'	2	−1	0	2	−1	0	x, y
A_1''	1	1	1	−1	−1	−1	
A_2''	1	1	−1	−1	−1	1	z
E''	2	−1	0	−2	1	0	R_x, R_y

Table 5.4: Character table of the $D_{3\mathrm{h}}$ point group.

The vibrational wave functions are nevertheless mainly localized at the minima of the potential energy surfaces corresponding to a $C_{3\mathrm{v}}$ geometry. In the $C_{3\mathrm{v}}$ point group, the electronic configuration of ammonia in the $\tilde{\mathrm{X}}$ ground electronic state is $(1\mathrm{a}_1)^2(2\mathrm{a}_1)^2(1\mathrm{e})^4(3\mathrm{a}_1)^2$. The lowest-lying electronically allowed transition corresponds to the excitation of an electron from the $3\mathrm{a}_1$ orbital, which is a nonbonding orbital (lone pair) of the nitrogen atom, into the diffuse 3s Rydberg orbital with a NH_3^+ planar ion core. In the electronically excited state, the molecule has a planar structure with $D_{3\mathrm{h}}$ point-group symmetry. In this point group, the excited electronic configuration and the electronic state are labeled $(1\mathrm{a}_1')^2(2\mathrm{a}_1')^2(1\mathrm{e}')^4(1\mathrm{a}_2'')^1(3\mathrm{sa}_1')^1$ $\tilde{\mathrm{A}}$ $^1\mathrm{A}_2''$.

The absorption spectrum of the $\tilde{\mathrm{A}} \leftarrow \tilde{\mathrm{X}}$ transition recorded using a room-temperature sample in which only the ground vibrational level of the $\tilde{\mathrm{X}}$ state is significantly populated is displayed in Figure 5.13. The spectrum consists of a single progression in the out-of-plane bending (umbrella) mode ν_2 of the $\tilde{\mathrm{A}}$ state. The origin band is labelled as 0_0^0 and the members of the progression as 2_0^n, indicating that the electronic transition originates in the vibrational ground state of the $\tilde{\mathrm{X}}$ state of ammonia and ends in the $v_2 = n$ vibrationally excited level of the $\tilde{\mathrm{A}}$ state. The weak band observed at lower wave numbers than the origin band is the hot band 2_1^0. The very long progression, extending beyond $n = 15$, is characteristic of a large

change in equilibrium geometry between the two electronic states involved in the transition.

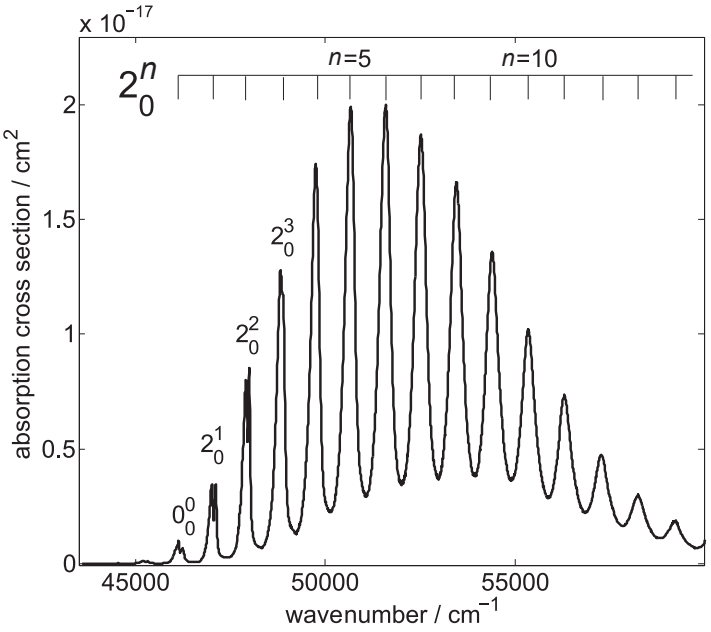

Figure 5.13: Absorption spectrum of the $\tilde{\mathrm{A}} \leftarrow \tilde{\mathrm{X}}$ transition of ammonia (data from B.-M. Cheng *et al.*, *Astrophys. J.*, **647**, 1535 (2006)). The origin of the electronic transition is labeled as 0_0^0 and the dominant progression in the out-of-plane bending mode ν_2 is labelled 2_0^n. The members of this progression originate in the vibrational ground state of the $\tilde{\mathrm{X}}$ state and end in the $v_2 = n$ level of the $\tilde{\mathrm{A}}$ excited state.

The simplest way to understand the fact that transitions to both even and odd vibrational levels are observed without noticeable intensity alternations between even and odd levels is to evaluate the selection rules in the $C_{3\mathrm{v}}$ point group (see table in Section 4.2.2). In this group, the electronic transition is allowed, and the umbrella mode is totally symmetric, so that the vibrational selection rule and intensity distribution can be described by the vibrational selection rule (5.63) and the Franck-Condon factors, respectively.

The vibrational intensity distribution can also be explained in the $D_{3\mathrm{h}}$ point group. However, in this group, the umbrella mode ν_2 is not totally symmetric, but of a_2'' symmetry. Consequently, one would predict on the basis of Equation (5.63) that the vibrational bands corresponding to odd values of the vibrational quantum number v_2 of the umbrella mode should be missing in an absorption spectrum from the ground vibrational level. The reason why transitions to vibrational levels with odd values of v_2 are observed is that they originate from the upper tunneling component of the ground state which has A_2'' vibronic symmetry (and thus may be regarded as the first excited vibrational level of the ground state).

Transitions to vibrational levels with even values of v_2 originate from the lower tunneling component of the ground state, which has A_1' symmetry. The two tunneling components are almost equally populated under the experimental conditions used to record the spectrum displayed in Figure 5.13, so that no intensity alternations in the ν_2 progression are observed. This example also served the purpose of illustrating some of the difficulties one encounters in interpreting electronic states with equilibrium structures corresponding to different point groups.

Electronically forbidden but vibronically allowed transitions

Electronically forbidden transitions may gain intensity from an allowed transition through vibronic coupling mediated by a non-totally-symmetric mode (the Herzberg-Teller effect), as discussed above.

A prototypical example of this situation is the electronically forbidden $\tilde{A}\ ^1B_{2u} \leftarrow \tilde{X}\ ^1A_{1g}$ transition of benzene (C_6H_6). This transition is also referred to as the $S_1 \leftarrow S_0$ transition, according to the nomenclature introduced in Section 5.1.3. The excited electronic state arises from the electronic configuration $(a_{2u})^2(e_{1g})^3(e_{2u})^1$ (showing the π molecular orbitals only). The direct product of the irreducible representations of the partially occupied orbitals is $E_{1g} \otimes E_{2u} = B_{1u} \oplus B_{2u} \oplus E_{1u}$, giving rise to the electronic states $^3B_{1u}$, $^1B_{1u}$, $^3B_{2u}$, $^1B_{2u}$, $^3E_{1u}$, and $^1E_{1u}$. In both the $\tilde{A}\ ^1B_{2u}$ and the $\tilde{X}\ ^1A_{1g}$ state, the benzene molecule has D_{6h} point-group symmetry. The dipole moment operator transforms as $A_{2u} \oplus E_{1u}$ and thus the only allowed electronic transitions originating from the ground electronic state end in states of electronic symmetry A_{2u} or E_{1u}. The $\tilde{A}\ ^1B_{2u} \leftarrow \tilde{X}\ ^1A_{1g}$ transition in benzene is thus forbidden, while the $\tilde{C}\ ^1E_{1u} \leftarrow \tilde{X}\ ^1A_{1g}$ transition is allowed (see Table 5.2). However, vibrational modes of symmetry $B_{2u} \otimes E_{1u} = E_{2g}$ induce vibronic coupling between the $\tilde{A}$ and $\tilde{C}$ electronic states.

Figure 5.14 shows a low-resolution overview spectrum of benzene in the region of 37000-42000 cm^{-1}, which was first analyzed in J. H. Callomon, T. M. Dunn and I. M. Mills, *Phil. Trans. Roy. Soc. A*, **259**, 499–532 (1966). The spectrum is dominated by a strong regular progression of absorption bands connecting the ground vibrational level of the $\tilde{X}$ state to vibrationally excited levels of the $\tilde{A}$ state. The nomenclature $1_0^n 6_0^1$ indicates that the lower level of the transition has the quantum numbers $v_1 = v_6 = 0$, *i. e.* both ν_1 and ν_6 are unexcited, whereas the upper level of the transition has $v_1 = n$ and $v_6 = 1$. The origin of the band system, designated as 0_0^0, does not carry intensity, as expected for an electronically forbidden

transition. The ν_1 and ν_6 vibrational modes have A_{1g} and E_{2g} symmetry, respectively, in both electronic states. The vibronic symmetry of the upper levels of the observed transition is thus $\Gamma_e \otimes \Gamma_v = B_{2u} \otimes [A_{1g}]^n \otimes E_{2g} = E_{1u}$ which can be accessed from the ground vibronic state through the E_{1u} component of the electric-dipole-moment operator (see Table 5.2).

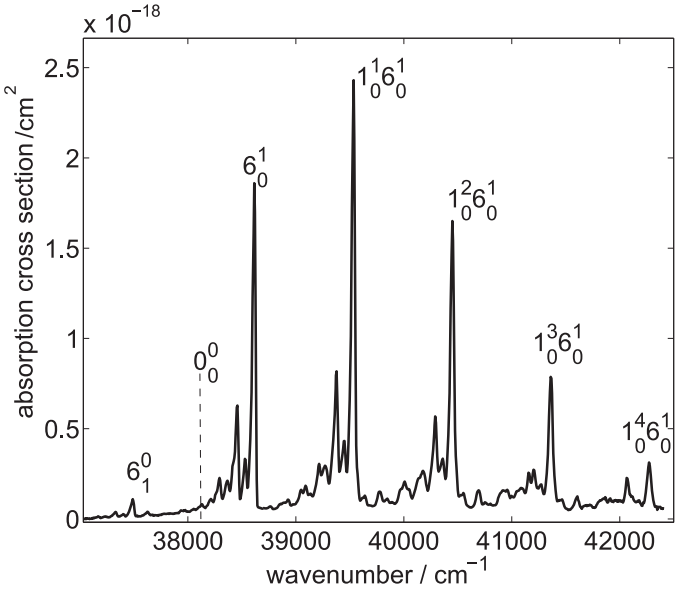

Figure 5.14: Low-resolution absorption spectrum of benzene in the 38000-42000 cm^{-1} region (data from T. Etzkorn *et al.*, *Atmos. Enivron.*, **33**, 525-540 (1999)). The transitions labelled $1_0^n 6_0^1$ originate from the vibrational ground state of the $\tilde{X}\ ^1A_{1g}$ state and end in the ($v_1 = n$,$v_6 = 1$) vibrational states of the $\tilde{A}\ ^1B_{2u}$ electronically excited state. The origin of the band (marked as 0_0^0) does not carry intensity. The vibronically allowed hot band 6_1^0 is observed below the origin band.

All strong transitions in this band system end in $v_6 = 1$ levels, which indicates that, among all vibrational modes of benzene, ν_6 is the mode primarily involved in mediating the vibronic interaction. Below the origin of the band, the weak transition labelled as 6_1^0 originates from the thermally populated $v_6 = 1$ vibrationally excited level of the ground electronic state and ends in the vibrational ground state of the $\tilde{A}\ ^1B_{2u}$ state. Such a transition is a hot band and is not observed when the vibrational temperature of the molecule is sufficiently low. One should note that the 6_1^0 band is vibronically allowed, which explains why it is observed, whereas transitions from other thermally populated excited vibrational levels of the ground state are not detected.